



Cite this: *Chem. Commun.*, 2019, 55, 14980

Received 18th October 2019,  
Accepted 19th November 2019

DOI: 10.1039/c9cc08174g

rsc.li/chemcomm

# A coumarin chalcone ratiometric fluorescent probe for hydrazine based on deprotection, addition and subsequent cyclization mechanism†

Miaomiao Xing,<sup>a</sup> Kangnan Wang,<sup>a</sup> Xiangwen Wu,<sup>b</sup> Shuyue Ma,<sup>a</sup> Duxia Cao,<sup>a</sup> Ruifang Guan<sup>✉</sup> and Zhiqiang Liu<sup>✉</sup><sup>\*c</sup>

**A ratiometric fluorescent probe for hydrazine based on a coumarin chalcone framework and a levulinic acid terminal group with a low detection limit (0.1 ppb, 0.003 μM), a large ratiometric fluorescence change ( $I_{465}/I_{575}$ , 1265-fold enhancement) and a wide pH work range (3.0–12.0) was developed. The mechanism analysis of the isolated hydrazine product characterized by NMR, HRMS and the crystal structure indicates that the levulinic acid group is firstly removed by deprotection and then the dihydropyrazole ring is formed due to the addition and subsequent cyclization reaction in the presence of hydrazine.**

Hydrazine (N<sub>2</sub>H<sub>4</sub>) has wide applications in fuels, in fuel cell reactors, even missile and rocket propulsion systems.<sup>1</sup> In addition, as a highly active alkali and strong reducing agent, it is also widely used in medicines and pesticides, such as anti-tuberculosis, anti-diabetes, and herbicides, and plant growth regulators. Meanwhile, hydrazine also plays a vital role in phase chemicals, emulsifiers, corrosion inhibitors and textile dyes.<sup>2</sup> However, hydrazine is highly toxic to organisms and seriously pollutes the environment and soil. Hydrazine also has excellent water solubility, which makes it easily absorbed by the body through the mouth or skin, causing serious damage to the organs and the central nervous system.<sup>3</sup> US Environmental Protection Agency (EPA) regards hydrazine as a potential carcinogen and its Threshold Limit (TLV) is set as 10 ppb.<sup>4</sup> Therefore, it is important to develop a reliable, real-time and sensitive method to detect hydrazine in small amounts.

Among the developed detection methods including electrochemical analysis,<sup>5</sup> capillary electrophoresis,<sup>6</sup> chromatography<sup>7</sup>

and so on, fluorescent probes are especially favored by researchers because of their sensitivity, convenience, excellent selectivity and harmless characteristics.<sup>8</sup> Traditional single-emission fluorescent probes are easily affected by the light intensity and optical path in quantitative detection.<sup>9</sup> By contrast, ratiometric fluorescent probes tend to be more advantageous, and their dual-emissive signals can effectively avoid the interference caused by fluctuation of excitation laser power and uneven dyeing, thus ratiometric fluorescent probes have more advantages in quantitative detection.<sup>10</sup> In addition, the ratiometric fluorescent probes can overcome the background signal by virtue of this advantage, so they have a huge advantage in biological imaging.<sup>11</sup>

Although fluorescent probes have great advantages in the detection of hydrazine, there are relatively few examples reported. Based on the literature reports on chemosensors for N<sub>2</sub>H<sub>4</sub> in recent years, they can be roughly divided into substituted,<sup>3c</sup> additive,<sup>1b,2a,3b,5</sup> and deprotected<sup>2b,c,3a,4,12</sup> fluorescent probes according to the recognition mechanism.<sup>13</sup> The most commonly used molecular group of deprotected fluorescent probes is the lipid group. Further cyclization mechanisms are scarcely involved.<sup>14</sup> Furthermore, most recognition mechanisms of fluorescence probes for analysts are based on *in situ* <sup>1</sup>H NMR,<sup>2c,3b,4,5,12a</sup> MS<sup>2a,12b,15</sup> and spectral change.<sup>16</sup> Though there are several probes for N<sub>2</sub>H<sub>4</sub>, whose response mechanisms are based on isolated products, a few can be proved by the crystal structure. The crystal structure of the product is the most direct proof for the mechanism, but it is often not obtained easily because of its instability and difficulty to purify.

Here, we report a novel ratiometric fluorescent probe for hydrazine based on a coumarin chalcone framework and levulinic acid terminal group, which can detect N<sub>2</sub>H<sub>4</sub> with high sensitivity. The mechanism analysis indicates that the elimination, addition and subsequent cyclization reaction are responsible for the recognition, which is proved by the crystal structure of the dihydropyrazole product for the first time. Compared with some reported chemosensors for hydrazine (Table S1, ESI†), the probe has excellent anti-interference, low detection limit (0.1 ppb, 0.003 μM), large ratiometric fluorescence change ( $I_{465}/I_{575}$ , 1265-fold enhancement)

<sup>a</sup> School of Materials Science and Engineering, University of Jinan, Jinan 250022, Shandong, China. E-mail: duxiacao@ujn.edu.cn, mse\_guanrf@ujn.edu.cn

<sup>b</sup> College of Chemistry, Chemical Engineering and Materials Science, Collaborative Innovation Center of Functionalized Probes for Chemical Imaging, Key Laboratory of Molecular and Nano Probes, Ministry of Education, Shandong Normal University, Jinan 250014, Shandong, China

<sup>c</sup> State Key Laboratory of Crystal Materials, Shandong University, Jinan 250100, Shandong, China. E-mail: zqliu@sdu.edu.cn

† Electronic supplementary information (ESI) available: Experimental procedures and supplemental spectra. CCDC 1955986 and 1955987. For ESI and crystallographic data in CIF or other electronic format see DOI: 10.1039/c9cc08174g

and importantly, the probe can detect hydrazine in an environment with a pH range of 3.0–12.0. The wide pH range overcomes the shortcoming that traditional fluorescent probes can only detect hydrazine in an acidic environment.

The compound was synthesized using diethylaminocoumarin-hydroxyl chalcone (**R-OH**) and levulinic acid as starting materials, 1-(3-dimethylaminopropyl)-3-ethylcarbodiimide hydrochloride (EDC) as a condensing agent, and 4-dimethylaminopyridine (DMAP) as a catalyst (Scheme S1, ESI<sup>†</sup>). It was characterized by NMR, high resolution mass spectra and the crystal structure (Fig. S1 and Table S2, ESI<sup>†</sup>).

The crystal belongs to the triclinic system and  $P2_1/c$  space group. The molecule has a certain planarity with the dihedral angle between coumarin moiety and terminal phenyl rings being  $36.21^\circ$  even the probe has a large substitute of the levulinic acid group (Fig. S3, ESI<sup>†</sup>). The molecule exhibits a slight charge transfer from diethylaminocoumarin to terminal phenyl rings (Fig. 1). In the packing diagram, layers are formed along the  $c$  axis and in each layer, the molecules are parallel to each other, the adjacent molecules along the  $b$  axis are arranged in a head-to-tail manner. In the nearest layers, the molecules are also aligned in a head-to-tail manner.

The solvent effect of the probe was tested and the corresponding UV-vis absorption and fluorescence spectra are shown in Fig. 2 and Fig. S4 (ESI<sup>†</sup>). In addition to hexane, probe **1** exhibits similar absorption spectra in other various organic solvents with a single absorption peak. The compound has two vibration absorption peaks at 420 nm ( $\epsilon = 6.8 \times 10^4 \text{ M}^{-1} \text{ cm}^{-1}$ ) and 440 nm ( $\epsilon = 6.7 \times 10^4 \text{ M}^{-1} \text{ cm}^{-1}$ ) in hexane (Fig. S4, ESI<sup>†</sup>). And with the increase of the organic solvent polarity, the absorption spectrum of compound **1** exhibits a pronounced red shift of 49 nm from hexane to water. The solvent polarity also has a great influence on the fluorescence spectra of probe **1**. The fluorescence peak position shows a significant red shift of 129 nm from hexane to water and the solution colour changes from blue to orange under 365 nm ultraviolet light. Except for *n*-hexane and water, probe **1** has strong

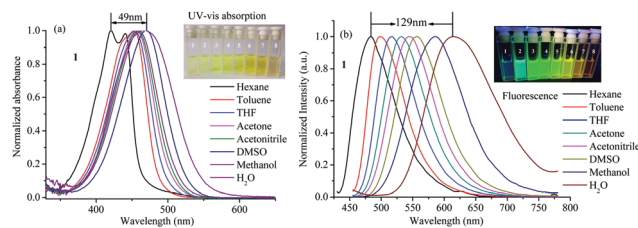


Fig. 2 Normalized UV-vis absorption (a) and fluorescence spectra (b,  $\lambda_{\text{ex}} = 420 \text{ nm}$ ) of probe **1** ( $10 \mu\text{M}$ ) in various solvents. Inset: Solution images of probe **1** in various solvents under natural light (a) and 365 nm UV light (b) (1-hexane, 2-toluene, 3-THF, 4-acetone, 5-acetonitrile, 6-DMSO, 7-methanol and 8- $\text{H}_2\text{O}$ ).

fluorescence emission in most solvents (Fig. S4, ESI<sup>†</sup>) with high quantum yields (toluene, 0.63; THF, 0.76; acetone, 0.75; acetonitrile, 0.68; DMSO, 0.52; methanol, 0.22). By adjusting the polarity of the solvent, luminescence from blue to orange can be realized. The larger solvent effect indicates that the probe has high polarity both in ground and excited states.

To study the recognizing properties of probe **1** toward hydrazine, UV-vis absorption and fluorescence titration experiments (Fig. 3) were conducted with 0.01 M hydrazine water solution in an aqueous solution of **1** ( $10 \mu\text{M}$ ,  $V_{\text{HEPES}}:V_{\text{DMSO}} = 1:4$ ,  $\text{pH} = 7.4$ ). It can be seen from Fig. 3a that with the addition of hydrazine, the absorption peak of the compound at 472 nm gradually decreases and is slightly red shifted. When hydrazine reaches 50 equiv., the red shift reaches a maximum of 15 nm, and its absorption peak appears at 487 nm. However, with the further increase of hydrazine, no red shift occurs, but the absorbance peak at 487 nm gradually decreases. Moreover, during the whole process of titration of hydrazine, a new peak at 388 nm appears and the absorbance is continuously enhanced. It reaches saturation when the number of equivalents of hydrazine is 110 equiv. According to the inset of Fig. 3a, the probe solution changes from yellow to colorless with

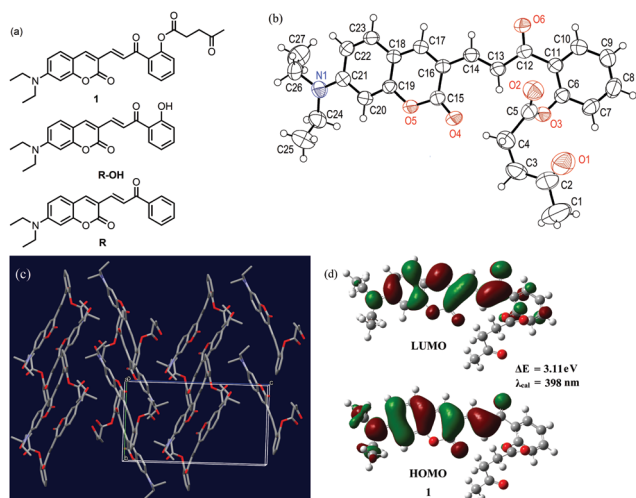


Fig. 1 Molecular structure of probe **1**, **R-OH** and **R** (a), X-ray molecular structure (b), packing diagram along  $a$  axis (c) and frontier molecular orbital HOMO and LUMO of the probe **1** (d).

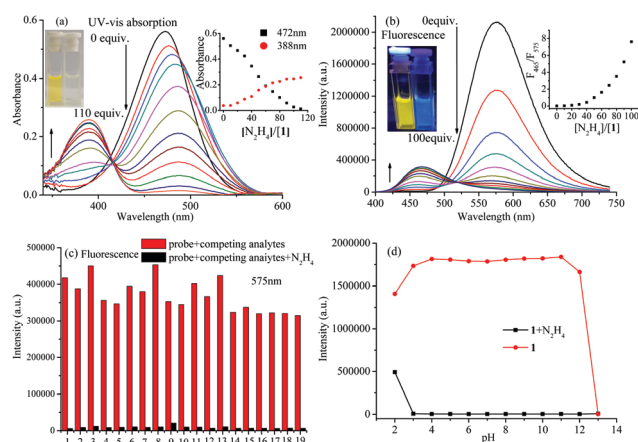


Fig. 3 UV-vis absorption (a), fluorescence (b) spectral changes, competitive selectivity (c, (1) **Probe**, **Probe** +  $\text{N}_2\text{H}_4$ ; (2)  $\text{NaClO}$ ; (3)  $\text{NaCN}$ ; (4)  $\text{NaCO}_3$ ; (5)  $\text{F}^-$ ; (6)  $\text{NaHSO}_3$ ; (7)  $\text{NaI}$ ; (8)  $\text{Na}_3\text{PO}_4$ ; (9)  $\text{Na}_2\text{S}$ ; (10)  $\text{NaCl}$ ; (11)  $\text{Na}_2\text{SO}_4$ ; (12)  $\text{NaSCN}$ ; (13)  $\text{NaBr}$ ; (14) urea; (15) bromoethylamine; (16)  $(\text{NH}_4)_2\text{S}$ ; (17) ethylenediamine; (18) propylamine; (19) butylamine) and pH dependence (d) of **1** ( $10 \mu\text{M}$ ) upon the addition of hydrazine in HEPES/DMSO (1:4, v/v),  $\lambda_{\text{ex}} = 380 \text{ nm}$ .

the addition of hydrazine, which means that the probe can act as a naked-eye probe for hydrazine in aqueous solution.

According to the inset of Fig. 3b, the probe solution itself exhibits a bright yellow fluorescence, which becomes blue with the addition of hydrazine. The fluorescence peak at 575 nm decreases with the addition of hydrazine, and at the same time, a new peak at 465 nm appears, and reaches the maximum at 100 equivalent.

The quantum yields of the probe in HEPES/DMSO (1:4, v/v) before and after the addition of hydrazine are 0.43 and 0.22, respectively. Moreover, when the equivalent number of hydrazine increases from 0 to 40 equiv., the fluorescence decreasing rate is significantly faster than that when adding 50 to 100 equiv. of hydrazine. The hydrazine fluorescence ratio  $I_{465}/I_{575}$  increases from 0.006 to 7.59 with 1265-fold enhancement. According to Fig. S5 (ESI<sup>†</sup>), the detection limit<sup>17</sup> can be calculated to be 0.1 ppb, which is far below the 10 ppb set by the EPA and lower than that of most reported chemosensors (Table S1, ESI<sup>†</sup>). According to UV-vis absorption and fluorescence titration, there seems to be a two-stage reaction.

In addition, the recognition time of the probe to hydrazine was explored (Fig. S6, ESI<sup>†</sup>). The probe completely reacts with hydrazine (100 equiv.) in 60 min. Therefore, 60 min was used as the recognition time in the subsequent experiments.

In order to investigate the sensing mechanism, the recognition effect of the precursor compound **R-OH** on hydrazine was also studied (Fig. S7, ESI<sup>†</sup>). The results indicate that the compound exhibits a similar recognition phenomenon for hydrazine, with the appearance of a new absorption peak at 388 nm accompanied by the disappearance of the original absorption peak at 487 nm, and a ratiometric fluorescent response with fluorescence ratio  $I_{465}/I_{575}$  showing 202-fold enhancement and 1.25 ppb of detection limit (Fig. S8, ESI<sup>†</sup>). Probe **1** has much higher recognition sensitivity than **R-OH**. The response time of compound **R-OH** with hydrazine is as long as 220 min (Fig. S9, ESI<sup>†</sup>), which is much longer than that of probe **1**. In combination with the absorption titration of probe **1**, it can be inferred that when 50 equiv. of hydrazine is added, the levulinic acid group of probe **1** is eliminated to afford compound **R-OH**, so that the absorption peak shows a red shift in the early stage of titration. Compound **R** without a hydroxyl group has a similar structure to **R-OH**. Compound **R** has no obvious recognition effect on hydrazine (Fig. S10, ESI<sup>†</sup>), which indicates that the hydroxyl group plays an important role in promoting the recognition process. By comparison of the above spectra, probe **1** has significant advantages in sensitivity, time response, and strong fluorescence emission compared to compound **R-OH**.

After comparison with the titration diagrams of **1** and **R-OH**, we believe that the reaction products of both the probes to hydrazine are identical. Moreover, according to the phenomenon that the peak position of compound **R-OH** is consistent with the linear pattern after the red shift in the preliminary titration spectra of probe **1**, it is believed that the levulinic acid group on probe **1** reacts with hydrazine to form a hydroxyl group at first. Excess hydrazine will be added to the carbon-carbon double bond and carbon-oxygen double bond on probe **1** and then further ring-forming reaction occurs,<sup>14d</sup> as shown in Fig. 4. The Job-plot point shows that the binding ratio of probe **1** to hydrazine is 1:1 (Fig. S11, ESI<sup>†</sup>).

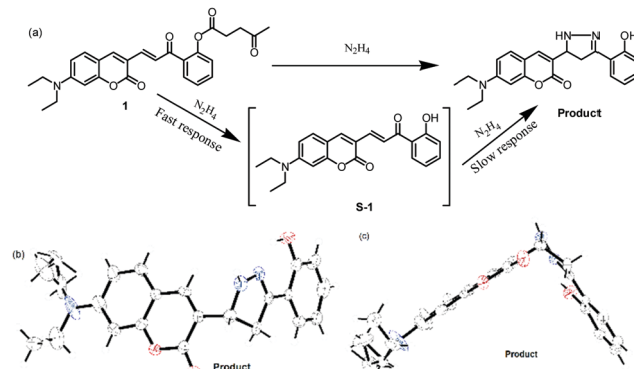


Fig. 4 The reaction mechanism diagram of probe **1** with hydrazine (a). Molecular structure (b) and planarity (c) of hydrazine **Product**.

In order to further clarify the recognition mechanism of probe **1** for hydrazine, the reaction **product** was successfully isolated and characterized by <sup>1</sup>H NMR, <sup>13</sup>C NMR, HRMS (Fig. S2, ESI<sup>†</sup>) and the crystal structure (Fig. 4b and c), which further proved the mechanism. The crystal structure clearly indicates the formation of the dihydropyrazole ring and the removal of levulinic acid. The reaction **product** exhibits the same absorption and fluorescence spectra with the probe after the addition of hydrazine (Fig. S12, ESI<sup>†</sup>). There is a serious twist between the coumarin moiety and terminal dihydropyrazole ring in the **product** structure, which limits the intramolecular charge transfer and the molecule mainly exhibits fluorescence emission from the coumarin group. DFT and TDDFT calculations were also carried out on the **product**. The calculated absorption (341 nm) is blue-shifted to that of probe **1** (398 nm), which is consistent with the experimental data.

In order to prove the selectivity and anti-interference of probe **1**, a competitive selectivity experiment was performed on probe **1**. As shown in Fig. 3c, the fluorescence of the probe does not change significantly when other analysts are added. Moreover, when other interfering ions and molecules are added, probe **1** and hydrazine can react normally. The above results indicate that probe **1** has excellent selectivity and anti-interference.

pH is an important factor affecting the reaction of the probe with hydrazine. Therefore, a pH-dependent test for probe identification was performed (Fig. 3d). The probe is found to be stable in the pH range of 3.0–12.0, and also exhibits excellent recognition properties in this range. This shows that pH has little effect on the probe, and the probe can achieve excellent recognition of hydrazine in this wide range, overcoming the limitation of the traditional hydrazine fluorescent probe which identifies hydrazine only in an acidic environment. As shown in Table S1 (ESI<sup>†</sup>), to the best of our knowledge, the reported widest pH work range is 5.0–10.0.

Due to the excellent spectral recognition properties of the probe to hydrazine, the application of probe **1** in the strip test of hydrazine was explored. As shown in Fig. S13 (ESI<sup>†</sup>), after exposing to hydrazine, the yellow-to-blue fluorescence transition of the strip, which was treated with the probe solution, occurred within 3 minutes. Meanwhile, its blue fluorescence increases significantly with the increasing of hydrazine concentration.

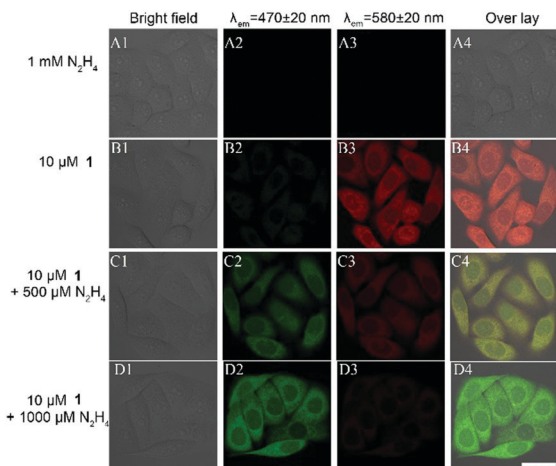


Fig. 5 Imaging of A549 cells with hydrazine (1 mM), compound **1** (10  $\mu$ M) before and after the addition of hydrazine ( $\lambda_{\text{ex}} = 405$  nm,  $\lambda_{\text{em}} = 470 \pm 20$  nm, pseudocolor green, green channel;  $\lambda_{\text{em}} = 580 \pm 20$  nm, pseudocolor red, red channel). Scale bar: 20  $\mu$ m.

To further develop the application of probe **1** in the detection of hydrazine in A549 cells and HeLa cells, a cytotoxicity test was firstly performed. As can be seen from the Fig. S14 (ESI<sup>†</sup>), when the probe concentration reaches 25  $\mu$ M, both A549 and HeLa cells still maintain a survival rate above 80%. As shown in Fig. 5, after adding 1 mM hydrazine to A549 cells, neither the green channel ( $\lambda_{\text{em}} = 470 \pm 20$  nm) nor the red channel ( $\lambda_{\text{em}} = 580 \pm 20$  nm) shows any fluorescent signal. When 10  $\mu$ M of probe **1** is added to A549 cells, the cells show a strong fluorescence signal in the red channel and an extremely weak fluorescence signal in the green channel. And when the cells are cultured with 10  $\mu$ M of probe **1** and 500  $\mu$ M of hydrazine, it is found that the fluorescent signal in the red channel is obviously attenuated, while the fluorescent signal in the green channel is significantly enhanced. After the concentration of hydrazine is further increased to 1000  $\mu$ M, the fluorescence signal in the red channel becomes extremely weak and almost disappears, while the fluorescence signal in the green channel is further strengthened, thereby achieving the identification of hydrazine in the cell.

In summary, based on the good photophysical properties of coumarin derivatives and their wide application in chemical sensing, coumarin chalcone compound **1** was developed. By comparing the recognition effects of compounds **R-OH**, **R** and **1** on hydrazine, we found that the substituted groups on the terminal benzene rings of compound **R-OH** (hydroxyl group) and **1** (levulinic acid group) can effectively promote the recognition of hydrazine. Moreover, compared with compound **R-OH**, probe **1** is more advantageous in terms of sensitivity, time response, and quantum yield. Based on the fact that probe **1** can recognize hydrazine in the range of pH 3.0–12.0 and has low cytotoxicity, we explored the application of the probe in cell imaging and found that it has a good recognition effect for hydrazine in biological cells.

This work was supported by the National Natural Science Foundation of China (21672130, 21601065), the Natural Science Foundation of Shandong Province (ZR2017MEM006), the Fundamental Research

Funds of Shandong University (2017JC011) and the State Key Laboratory of Crystal Materials.

## Conflicts of interest

There are no conflicts to declare.

## Notes and references

- (a) D. Cao, Z. Liu, P. Verwilst, S. Koo, P. Jangili, J. S. Kim and W. Lin, *Chem. Rev.*, 2019, **119**, 10403; (b) L. Cui, C. Ji, Z. Peng., L. Zhong, C. Zhou., L. Yan, S. Qu, S. Zhang, C. Huang, X. Qian and Y. Xu, *Anal. Chem.*, 2014, **86**, 4611.
- (a) X. Dai, Z.-Y. Wang, Z.-F. Du, J.-Y. Miao and B.-X. Zhao, *Sens. Actuators, B*, 2016, **232**, 369; (b) C. Hu, W. Sun, J. Cao, P. Gao, J. Wang, J. Fan, F. Song, S. Sun and X. Peng, *Org. Lett.*, 2013, **15**, 4022; (c) X. Xia, F. Zeng, P. Zhang, J. Lyu, Y. Huang and S. Wu, *Sens. Actuators, B*, 2016, **227**, 411.
- (a) M. G. Choi, J. Hwang, J. O. Moon, J. Sung and S.-K. Chang, *Org. Lett.*, 2011, **13**, 5260; (b) X.-X. Zhao, J.-F. Zhang, W. Liu, S. Zhou, Z.-Q. Zhou, Y.-H. Xiao, G. Xi, J.-Y. Miao and B. X. Zhao, *J. Mater. Chem. B*, 2014, **2**, 7344; (c) Y. Liu, D. Ren, J. Zhang, H. Li and X.-F. Yang, *Dyes Pigm.*, 2019, **162**, 112; (d) X. Gu and J. P. Camden, *Anal. Chem.*, 2015, **87**, 6460.
- X. Shi, F. Huo, J. Chao, Y. Zhang and C. Yin, *New J. Chem.*, 2019, **43**, 10025.
- R. Madhu, V. Veeramani and S.-M. Chen, *Sens. Actuators, B*, 2014, **204**, 382.
- J. Liu, W. Zhou, T. You, F. Li, E. Wang and S. Dong, *Anal. Chem.*, 1996, **68**, 3350.
- W. E. Davis and Y. Li, *Anal. Chem.*, 2008, **80**, 5449.
- (a) Y. Yue, F. Huo, P. Ning, Y. Zhang, J. Chao, X. Meng and C. Yin, *J. Am. Chem. Soc.*, 2017, **139**, 3181; (b) J. Yan, J. Zhu, K. Zhou, J. Wang, H. Tan, Z. Xu, S. Chen, Y. Lu, M. Cui and L. Zhang, *Chem. Commun.*, 2017, **53**, 9910; (c) J.-T. Hou, J. Yang, K. Li, Y.-X. Liao, K.-K. Yu, Y.-M. Xie and X.-Q. Yu, *Chem. Commun.*, 2014, **50**, 9947; (d) J. Wang, W. Xu, Z. Yang, Y. Yan, X. Xie, N. Qu, Y. Wang, C. Wang and J. Hua, *ACS Appl. Mater. Interfaces*, 2018, **10**, 31088; (e) Q. Hu, W. Li, C. Qin, L. Zeng and J. Hou, *J. Agric. Food Chem.*, 2018, **66**, 10913.
- X. Liu, L. Wang, T. Bing, N. Zhang and D. Shangguan, *ACS Appl. Bio Mater.*, 2019, **2**, 1368.
- (a) M. Santra, B. Roy and K. H. Ahn, *Org. Lett.*, 2011, **13**, 3422; (b) D. Song, S. Cho, Y. Han, Y. You and W. Nam, *Org. Lett.*, 2013, **15**, 3582.
- (a) K. Wang, Y. Zhu, M. Xing, D. Cao, R. Guan, S. Zhao, Z. Liu and Z. Mao, *Sens. Actuators, B*, 2019, **295**, 215; (b) L. Yuan, W. Lin, B. Chen and Y. Xie, *Org. Lett.*, 2012, **14**, 432; (c) Y. Zhu, K. Wang, W. Song, B. Dong, S. Zhao, R. Guan, Z. Li, Y. Sun, D. Cao and W. Lin, *Sens. Actuators, B*, 2019, **294**, 283.
- (a) K. Li, H.-R. Xu, K.-K. Yu, J.-T. Hou and X.-Q. Yu, *Anal. Methods*, 2013, **5**, 2653; (b) Y.-Z. Ran, H.-R. Xu, K. Li, K.-K. Yu, J. Yang and X.-Q. Yu, *RSC Adv.*, 2016, **6**, 111016; (c) X.-R. Shi, C.-X. Yin, Y.-B. Zhang, Y. Wen and F.-J. Huo, *Sens. Actuators, B*, 2019, **285**, 368; (d) J. Li, Y. Cui, C. Bi, S. Feng, F. Yu, E. Yuan, S. Xu, Z. Hu, Q. Sun, D. Wei and J. Yoon, *Anal. Chem.*, 2019, **91**, 7360; (e) C. Liu, K. Liu, M. Tian and W. Lin, *Spectrochim. Acta, Part A*, 2019, **212**, 42; (f) X. Shi, C. Yin, Y. Wen, Y. Zhang and F. Huo, *Spectrochim. Acta, Part A*, 2018, **203**, 106.
- (a) K. H. Nguyen, Y. Hao, W. Chen, Y. Zhang, M. Xu, M. Yang and Y.-N. Liu, *Luminescence*, 2018, **33**, 816; (b) Y. Jung, I. G. Ju, Y. H. Choe, Y. Kim, S. Park, Y.-M. Hyun, M. S. Oh and D. Kim, *ACS Sens.*, 2019, **4**, 441.
- (a) X. Shi, F. Huo, J. Chao and C. Yin, *Sens. Actuators, B*, 2018, **260**, 609; (b) S. Goswami, S. Das, K. Aich, D. Sarkar and T. K. Mondal, *Tetrahedron Lett.*, 2014, **55**, 2695; (c) Y.-H. Xiao, G. Xi, X.-X. Zhao, S. Zhou, Z.-Q. Zhou and B.-X. Zhao, *J. Fluoresc.*, 2015, **25**, 1023; (d) H. Wang, Y. Li, S. Yang, H. Tian, Y. Liu and B. Sun, *J. Photochem. Photobiol., A*, 2019, **377**, 36.
- (a) Y. He, Z. Li, B. Shi, Z. An, M. Yu, L. Wei and Z. Ni, *RSC Adv.*, 2017, **7**, 25634; (b) S. Chen, P. Hou, J. Wang, L. Liu and Q. Zhang, *Spectrochim. Acta, Part A*, 2017, **173**, 170.
- (a) Z. Li and K. S. Suslick, *Angew. Chem., Int. Ed.*, 2019, **58**, 14193; (b) Z. Li and K. S. Suslick, *ACS Sens.*, 2018, **3**, 121.
- (a) M. Zhu, M. Yuan, X. Liu, J. Xu, J. Lv, C. Huang, H. Liu, Y. Li, S. Wang and D. Zhu, *Org. Lett.*, 2008, **10**, 1481; (b) J. Isaad and A. E. Achari, *Tetrahedron*, 2011, **67**, 5678.